

## A model for complex aftershock sequences

Y. Moreno,<sup>1,2</sup> A. M. Correig,<sup>3</sup> J. B. Gómez,<sup>4</sup> and A. F. Pacheco<sup>1</sup>

**Abstract.** The decay rate of aftershocks is commonly very well described by the modified Omori law,  $n(t) \propto t^{-p}$ , where  $n(t)$  is the number of aftershocks per unit time,  $t$  is the time after the main shock, and  $p$  is a constant in the range  $0.9 < p < 1.5$  and usually close to 1. However, there are also more complex aftershock sequences for which the Omori law can be considered only as a first approximation. One of these complex aftershock sequences took place in the eastern Pyrenees on February 18, 1996, and was described in detail by *Correig et al.* [1997]. In this paper, we propose a new model inspired by dynamic fiber bundle models to interpret this type of complex aftershock sequences with sudden increases in the rate of aftershock production not directly related to the magnitude of the aftershocks (as in the epidemic-type aftershock sequences). The model is a simple, discrete, stochastic fracture model where the elements (asperities or barriers) break because of static fatigue, transfer stress according to a local load-sharing rule and then are regenerated. We find a very good agreement between the model and the Eastern Pyrenees aftershock sequence, and we propose that the key mechanism for explaining aftershocks, apart from a time-dependent rock strength, is the presence of dynamic stress fluctuations which constantly reset the initial conditions for the next aftershock in the sequence.

### 1. Introduction

*Omori* [1894] discovered scaling in earthquakes in the frequency distribution of aftershocks over 100 years ago when he proposed a formula to represent the decay of aftershock activity with time. Now, 100 years later, it remains as one of the few well-established empirical laws in seismology. As noted by *Utsu* [1995, p. 1], “any theory for the origin of aftershocks must explain this law, which is unique for its power law dependence on time”. The Omori law (as modified by *Utsu* [1961]),

$$n(t) = Kt^{-p}, \quad (1)$$

says that the number of aftershocks  $n(t)$ , measured at time  $t$  after the time of the main shock, declines following a power law with an exponent  $p$  around one ( $0.9 < p < 1.5$ , with a median of about 1.1 [*Utsu*, 1995]),

and  $K$  being a proportionality constant. To avoid divergence at  $t = 0$ , the Omori law is usually written in the form

$$n(t) = K(t + c)^{-p}, \quad (2)$$

where  $c$  is an additional “small” positive constant with dimensions of time (between 0.01 and 1 days, with a median of 0.3 days [*Utsu*, 1995]). The power law, scale-free behavior is maintained for  $t \gg c$ , with a transition to  $n(t) = \text{const}$  for  $t \leq c$  that accounts for incompleteness in the detection of low-magnitude aftershocks during the few hours after the mainshock [e.g., *Utsu*, 1995, Figure 2; *Gross and Kisslinger*, 1994]. From (2) the cumulative number of aftershocks,  $N(t)$ , occurred until time  $t$  after the main shock, defined as  $\int_0^t n(s)ds$ , is

$$N(t) = \begin{cases} K \ln(t/c + 1) & p = 1 \\ K \{c^{1-p} - (t + c)^{1-p}\} / (p - 1) & p \neq 1 \end{cases} \quad (3)$$

The Omori law has also been verified in laboratory-scale experiments in brittle rock deformation by measuring acoustic emission [*Scholz*, 1968a, 1968b; *Lockner and Byerlee*, 1977; *Hirata*, 1987; *Sammonds et al.*, 1992; *Lockner*, 1993] and in mine-induced seismicity [*Talebi*, 1997], which represents an intermediate scale between laboratory experiments and natural aftershocks. The fulfilment of the Omori law at the microscale ( $10^{-3}$ – $10^{-1}$  m), mesoscale ( $1$ – $10^1$  m) and macroscale ( $10^2$ – $10^4$  m), suggests that a universal process is behind the inelastic strain responsible for acoustic emission in the

<sup>1</sup>Departamento de Física Teórica, Universidad de Zaragoza, Zaragoza, Spain.

<sup>2</sup>Now at The Abdus Salam International Centre for Theoretical Physics, Condensed Matter Group, Trieste, Italy.

<sup>3</sup>Departament d’Astronomia i Meteorologia, Universitat de Barcelona, Barcelona, Spain.

<sup>4</sup>Departamento de Ciencias de la Tierra, Universidad de Zaragoza, Zaragoza, Spain.

laboratory [Hirata, 1987], induced microseismicity in mines [Gibowicz, 1997], and aftershock sequences in active tectonic faults [Utsu, 1995; Gross and Kisslinger, 1994]. However, what is this mechanism?

Static fatigue, also known as stress, creep, or delayed fracture is the basic way of time-dependent failure under a constant load of a broad variety of materials, including textile fibers [Coleman, 1957], fiber composites [Phoenix, 1977], wood [Garcimartín et al., 1997], microcrystals [Pauchard and Meunier, 1993], gels [Bonn et al., 1998], polycrystalline ceramics [Jacobs and Chen, 1994], metals [Schleinkofer et al., 1996], silicate glasses [Charles, 1958], minerals [Scholz, 1968a; Barnett and Kerrich, 1980], and rocks [Atkinson, 1984]. In all these cases, the signature of static fatigue is the observation of a failure strength that is a function of the load history of the material. For brittle materials, and from the point of view of fracture mechanics, time-dependent strength is commonly associated with kinetic fracture, *i.e.*, with the propagation of cracks under a crack tip stress intensity factor below the modulus of cohesion of the material [Kostrov et al., 1969]. This propagation is stable and quasi-static and is referred to as subcritical crack growth, where “quasi-static” means at velocities much less than the sonic velocity of the medium [Das and Scholz, 1981]. The presence of a chemically active fluid environment saturating the pore and crack space enhances this subcritical crack growth, a mechanism known as stress corrosion [Charles, 1958; Wiederhorn, 1967]. There is ample evidence that geological materials under brittle conditions owe their time-dependent strength to the mechanism of subcritical crack growth assisted by stress corrosion [Atkinson, 1984; Atkinson and Meredith, 1987].

Benioff [1951] presented the first detailed theory offering an explanation of the causes and characteristics of aftershock sequences in terms of identifiable mechanical properties. According to his theory, aftershocks occur when there is a time-dependent recovery of stress following the main shock. The stress recovery was ascribed by Benioff to a static fatigue of the rocks in the immediate area of the fault.

Since Benioff’s seminal paper, many laboratory and numerical experiments have confirmed the hypothesis that aftershocks are a process of relaxing stress concentrations produced by the dynamic rupture of the main shock and that they are therefore an intrinsic time-dependent rheological effect. In this context, Scholz [1968b] formulated the first time-dependent strength model of aftershocks. He suggested that a time-dependent strength of the rocks in the area of the main shock could be the cause of the aftershock sequences and invoked static fatigue due to local overloads to stresses much higher than their long-term strength as the main mechanism of aftershocks. On the basis of Scholz’s [1968a] laboratory experiments on static fatigue of quartz, Das and Scholz [1981] formulated a general model of aftershocks using elastic fracture mechan-

ics and the concept of subcritical crack growth. They showed that this model is consistent with the decay rate of aftershocks as expressed by the Omori law and that it is able to reproduce many other characteristics of real aftershock sequences. More recent works and papers that stress the role of time-dependent strength in aftershock dynamics are those by Yamashita and Knopoff [1987], who assumed that stress corrosion is the physical mechanism for the delayed fracture in aftershocks; Marcellini [1995, 1997], who advocated static fatigue, together with stress inhomogeneities, as the cause of Omori-law aftershock sequences; and Lee [1999] and Lee and Sornette [2000], who constructed a fuse network model of aftershocks incorporating a time-dependent strength compatible with the mechanism of subcritical crack growth. All these models of aftershocks also obey the Omori law.

As mentioned above, the Omori law decay rate of aftershocks following a main shock is an almost universal characteristic of seismicity (as compared to the more irregular patterns of premonitory activity as foreshocks or quiescence). However, despite this universality, many real aftershock sequences display anomalies in the decay rate that depart from the simple Omori law behavior. Among these anomalies we can cite [Utsu, 1995]: (1) cases in which seismic activity following the main shock cannot be represented by a simple power law due to the mixing of different series of activity [Gross and Kisslinger 1994]; and (2) cases where aftershocks decay, as a whole, according to the Omori law but depart temporarily from the formula due to abrupt changes in activity (accelerations and/or quiescence).

In this paper we are interested in aftershock series that do not rigorously follow the Omori law and, in particular, in this second type of anomalies where sudden accelerations in the rate of aftershock activity are not directly linked to aftershocks of larger magnitude. This last case is the so-called epidemic-type aftershock sequence (ETAS), where each aftershock has its own sequence of aftershocks [Ogata, 1988], and can be thought of as a fractal version of the simple Omori relaxation formula. There are, however, some aftershock sequences where the changes in decay rate are independent of the magnitude of the aftershocks that provoke these changes in activity, and that cannot be ascribed to the ETAS model. One of these aftershock sequences took place in the eastern Pyrenees on February 18, 1996 [Correig et al., 1997] and in this paper we propose a simple stochastic model á la dynamic fiber bundle model as a framework to interpret this class of aftershock sequences.

## 2. Data

On February 18, 1996, a local magnitude  $M_L = 5.2$  earthquake occurred in the eastern Pyrenees, with epicentral location  $42^\circ 47.71'N$ ,  $2^\circ 32.30'E$  and focal depth of 8 km [Rigo et al., 1997; Pauchet et al., 1999].

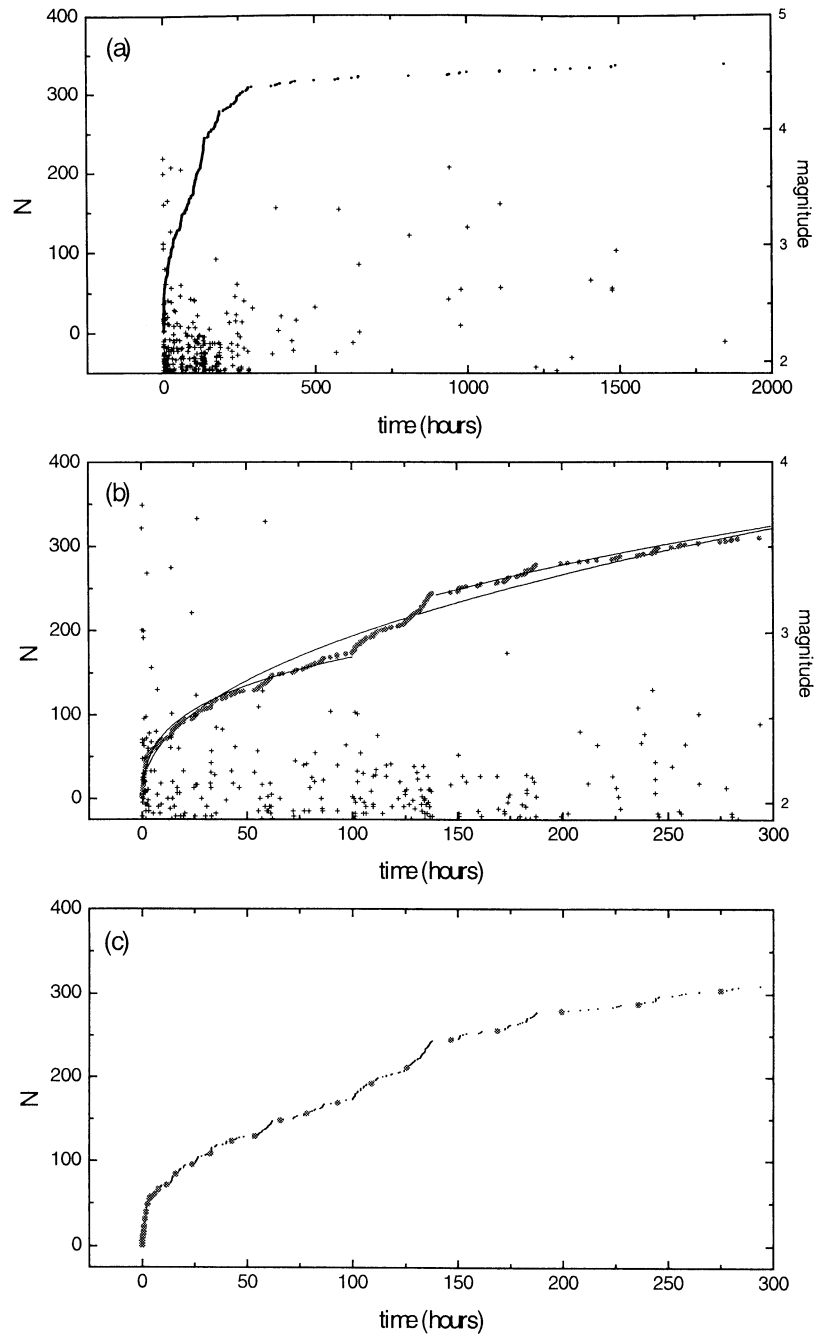


**Figure 1.** Aftershock sequence of February 18, 1996, eastern Pyrenees. (a) Complete series of aftershocks, shown as the accumulated number of events (left axis), together with their magnitude (right axis). (b) First 300 hours of the aftershock sequence, as used in the comparison with the model results. The fit to the whole range and two independent fits to the 0-100 and 140-300 hours intervals has been superimposed. (c) Separation of the aftershock sequence into leading aftershocks (solid circles) and cascade events (dots). See the text for details.

The series of aftershocks that followed this event was recorded at the three-component continuous broadband seismic station at the Tunel del Cadí, located at  $\sim 80$  km SW of the epicentral area. Altogether, the series consists of 337 events (complete for a threshold magnitude of 1.9), spanning 1846 hours (77 days) from the time of the main shock, and with magnitudes ranging

from 1.9 to 3.8. Figure 1a shows the cumulative series of aftershocks, along with the magnitude of the events. The sudden change in slope at  $\sim 300$  hours is not due to incompleteness of the series, and from the point of view of the magnitude of the aftershocks, there is no specific characteristic, nor any relevant event, that justifies this sudden change in the event rate. Because of

this different behavior we will restrict our attention to the series defined by the first 300 hours, with a total of 308 events, as displayed in Figure 1b.

The most striking feature of this series is the change in concavity of the cumulative curve not correlated to any significant event (as would be the case from the point of view of an ETAS model), suggesting an increase in the rate of aftershocks production apparently not related to any relaxation process. If we try to fit by the maximum likelihood method the aftershock data in Figure 1b to (3), we immediately appreciate that a unique fit to the whole range (0-300 hours) is graphically worse than two independent fits to the ranges 0-100 and 140-300 hours. Unfortunately, the parameter estimation for the 140-300 hours is not unique in the sense that more than one set of parameter values return the same value of the likelihood function after maximization. After fixing the values of  $K$  and  $c$  (to the values  $K = 17 \pm 2$  and

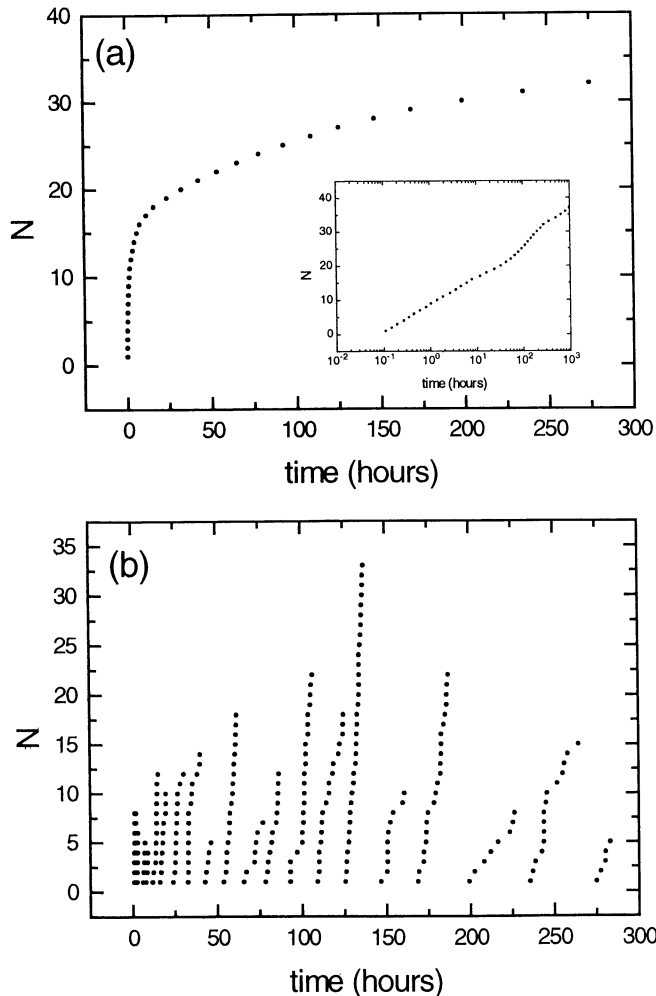


**Figure 2.** (a) Series formed by the leading aftershocks, after removal from the original sequence the cascades. The fit to the Omori law is much better than the original, and the  $p$  value (0.94) is also closer to worldwide aftershock  $p$  values. (b) Cascades retrieved from the original first 300 hours of the aftershock sequence. Each cascade can be approximated by a straight line.

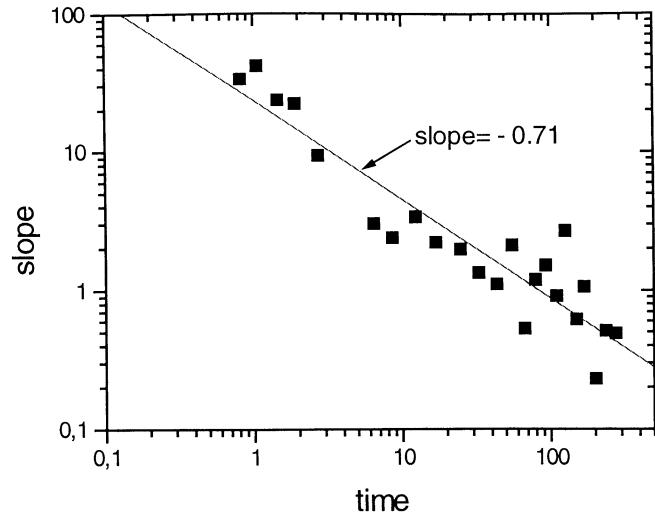


**Figure 3.** Slope of the cascades versus time on log-log scale. It can be clearly seen that it follows a power law  $s \propto t^{-\nu}$ , with  $\nu \approx 0.7$

$c = 0.2 \pm 0.1$  obtained for the fit to the 0-100 hour interval), the 140-300 hour fit returns a unique value for the parameter  $p = 0.654 \pm 0.005$ , which is statistically different to the value  $p = 0.75 \pm 0.04$  obtained for the 0-100 hour interval. The error in both estimates is one standard deviation assuming a normal distribution for the variance. These values of  $p$  are abnormally low (0.75 for the 0-100 hours interval, and 0.65 for the 140-300 hours interval). The fit and the value of  $p$  do not improve if the magnitude threshold is increased [Correig *et al.*, 1997].

The interpretation of the Omori law as a relaxation process suggests a way of separating the aftershocks in the series into two classes: class A for the events that follow a relaxation law and class B for those events that do not. The criterion to assign the events to classes A or B is the following: If the interval of time  $\Delta t_i$  between events  $i$  and  $i-1$  is strictly larger than the interval of time  $\Delta t_{i-1}$  between events  $i-1$  and  $i-2$ , the event  $i$  belongs to class A; otherwise, it belongs to class B. Events belonging to class A are termed leading aftershocks, and those belonging to class B are termed cascades. Figure 1c shows the aftershock sequence classified as leading events (solid circles) and cascades (dots). Note that a cascade is initiated by a leading aftershock and that this leading aftershock has no significant different magnitude.

The fit of (3) to the series formed by the leading aftershocks is shown in Figure 2a. The fit has improved significantly from the initial fit to the whole sequence, and the value obtained for the exponent is now  $p = 0.94$ , much more in agreement with the standard values for worldwide aftershock sequences. Figure 2b depicts the series of cascades, in which the first term of each cascade is a leading aftershock. Two important features are readily visible from Figure 2b: (1) the cascades are, in general, well approximated by straight lines; and (2)

their corresponding slopes decrease with time. A plot of the slope  $s$  of the cascades against time  $t$  (Figure 3) shows the remarkable fact that there exists a power law relationship of the form  $s \propto t^{-\nu}$  between them, with  $\nu \approx 0.71$ .

The properties summarized in Figures 1-3 for the aftershock sequence of the eastern Pyrenees can be described at first order with the modified Omori law, (Equations (2) and (3)). However, at second order, there are important nonrandom fluctuations about this law (represented by the cascades) that can not be fitted in detail with, nor accounted for, the Omori law and its relaxation origin. In Section 3 we will construct a model to account for this second-order deviations from the Omori law and for the Omori law itself, of course.

We want to stress here that the characteristics of the series of aftershocks from the February 18, 1996, Pyrenees main shock are by no means "exceptional". On the contrary, they seem to be a rather general feature of aftershock series. We are currently analyzing various aftershock sequences (Greece, Kobe, Landers, Northridge) and have found a behavior very similar to that of the Pyrenees aftershock sequence. Results will be reported elsewhere.

### 3. Dynamic Fiber Bundle Models

Fiber bundle models (FBMs) are simple discrete stochastic fracture models amenable to either close analytical or fast numerical solution. These models arose in intimate connection with the strength of bundles of textile fibers [Daniels, 1945; Coleman, 1957]. Since Daniels' and Coleman's seminal works, there has been a long tradition in the use of these simple models to analyze failure of heterogeneous materials [Vazquez-Prada et al., 1999, and references therein].

The dynamic version of the FBM simulates the failure of materials because of static fatigue or delayed rupture. In this version, one considers the following characteristics: (1) a discrete set of  $N$  elements located on the sites of a  $d$ -dimensional lattice; (2) a probability distribution for the nominal lifetimes of individual elements; and (3) a load transfer rule, which determines how the load carried by a failed element is to be distributed among the surviving elements in the set.

As stated in characteristic 2, the nominal lifetimes,  $t_j$ , of the individual elements supporting an initial stress  $\sigma_i$ , equal for all  $j$ , are taken from a probability distribution of the type

$$n_j = 1 - e^{-k(\sigma_i)t_j} \quad j = 1, 2, \dots, N, \quad (4)$$

where  $n_j$  are random numbers ( $0 \leq n_j \leq 1$ ) and  $k(\sigma_i)$  is the so-called hazard rate or breaking rule. The most accepted hazard rate is of the form

$$k(\sigma_i) = \nu_0 \left( \frac{\sigma_i}{\sigma_0} \right)^\rho, \quad (5)$$

$\nu_0$  and  $\sigma_0$  represent a hazard rate of reference and a stress of reference, respectively, and  $\rho$  is an exponent in the range  $2 < \rho < 50$ . This function has been used to fit experimental results of time to failure on various materials [Coleman, 1957; Phoenix, 1977]. Besides, Phoenix and Tierney [1983] derived it from a kinetic theory of thermally activated atomic bond rupture [Zhurkov, 1965] and showed that in many circumstances it is a better approximation than the exponential breaking rule,  $\kappa(\sigma) = \alpha \exp(\beta\sigma)$ , also used in modeling time-dependent fracture [Coleman, 1957].

Equation (5) has the same form as the Charles power law to describe stress corrosion induced subcritical crack growth in geological materials [Atkinson, 1984]:

$$v = v_0 \exp(-H/RT) K_I^n, \quad (6)$$

where  $v$  is the crack velocity,  $H$  is the activation energy,  $R$  is the gas constant,  $T$  is the absolute temperature,  $K_I$  is the stress intensity factor for mode I fracture, and  $v_0$  and  $n$  are constants. Sometimes,  $n$  is known as the stress corrosion index. Nominal values at room temperature and in wet rock are [Atkinson and Meredith, 1987]: 15-40 for quartz and quartz rocks; 10-30 for calcite rocks; 30-70 for granitic rocks; and 25-50 for gabbro and basalt. If we assume constant temperature, (6) can be simplified to

$$v = AK_I^n, \quad (7)$$

which is identical to (5) if we substitute  $\sigma$  by  $K$  and identify the breaking rate expressed by (5) with the crack opening velocity expressed by (7).

In dynamic FBMs, once elements begin to fail because of fatigue and their stress is transferred according to the assumed rule, the stresses among the surviving elements are no longer equal and the stress history of an individual element becomes complicated by the successive step-like transfers coming from failing elements. The effect of the increase in stress for a particular element  $j$  is the reduction of its lifetime from the initially assigned  $t_j$  to a  $T_j$  defined by

$$t_j = \int_0^{T_j} \left( \frac{\sigma_j(t)}{\sigma_i} \right)^\rho dt. \quad (8)$$

Notice that in the case of independent elements (i.e., no stress transfer),  $\sigma_j(t) = \sigma_i \forall j$  and hence the bundle would break as a succession of individual failures at the times  $t_j$  assigned at the beginning. When, on the contrary, stress redistribution between elements is assumed, the temporal series of individual failures actually occurs at the times  $T_j$  dictated by (8).

Note that in these models the total stress acting on the system is conserved until the failure of the last element; and for the reasons explained above, the last element, i.e., that with the longest  $T_j$ , does not coincide, in general, with that with the longest  $t_j$ . A detailed explanation of how to perform a Monte Carlo simulation

using this model is given by *Newman et al.* [1995], to which the reader is referred to for details.

The dynamic FBM can also be calculated using a probabilistic approach. This approach was introduced by us in the work by *Gómez et al.* [1998]. From this perspective, one starts with  $N$  elements loaded with an initial common stress equal to  $\sigma_i$ . The mean time interval,  $\delta$ , for one element to break by fatigue is

$$\delta = \frac{1}{\sum_{j=1}^N k(\sigma_j)}. \quad (9)$$

Supposing that  $\nu_0 = 1$  and  $\sigma_0 = 1$  in (5), we have

$$\delta = \frac{1}{\sum_{j=1}^N \sigma_j^\rho}, \quad (10)$$

In the first step,  $\sigma_j = \sigma_i \forall j$  and hence  $\delta = 1/N\sigma_i^\rho$ . This will change with time because of stress transfers. At any instant of the process of breaking,  $\delta$  of (10) represents the mean time for the next individual failure. The identification of which element breaks after one  $\delta$  is calculated by deciding that the probability that precisely element  $k$  be the affected one is given by

$$p_k = \sigma_k^\rho \delta. \quad (11)$$

The reader will note that from the probabilistic perspective, one does not consider weak elements or strong elements: Here all elements are equal but, in general, with a different  $\sigma_j$ . The succession of individual breakings proceeds by chance with the probabilities dictated by (11) until the total collapse of the system. *Gómez et al.* [1998] showed that the probabilistic approach represents a way of partially smoothing the fluctuations inherent to these stochastic models of fracture.

#### 4. Model

The model used in this paper to describe aftershock sequences is based on the same physical mechanism as the model recently introduced by *Lee* [1999] and *Lee and Sornette* [2000], although the ingredients of the cellular automaton, the way of running the model and the type of results are different. Our model is inspired by dynamic FBMs but with several substantive differences. As stated above, in dynamic FBMs,  $N$  uniformly loaded elements break by fatigue one after one, in a total stress conserving process until the last individual failure. The sequence always occurs in a finite time accelerated process.

Trying to describe a sequence of aftershocks, which is a clearly decelerated process of relaxation, we will modify three things.

1. Stress is lost in the breaking process in two ways: (1) by stress transfers out of the system through the borders, and (2) by considering a dissipative effect during each transfer: When an element fails bearing a stress  $\sigma$ , the fraction  $(1 - \pi)\sigma$  is removed from the system. Thus the constant  $\pi$  will represent the degree of conservation.

2. In FBMs, when an element fails, it transfers its load and then remains inactive. In this model, on the contrary, when an element fails, it transfers its load (except the dissipated fraction) to its nearest neighbors, but then it is automatically regenerated and able to receive stress again and actively participate in the time evolution of the set. After its regeneration, an element has zero load before receiving any load. This assumption is justified because time intervals between individual failures are much longer than the time of actual breaking of an asperity, and hence in an interevent interval a just failed asperity has enough time to heal.

3. The third modification to standard FBMs is related to the initial stress distribution in the system. While in FBMs it is usually assumed that the initial load per element is a constant  $\sigma_i$ , here, trying to simulate the disordered state existing in the fault after a main shock, we will take the initial  $\sigma_j$  from a uniform probability distribution ( $0 \leq \sigma_j < 1; 1 \leq j \leq N$ ). In the actual running of the model we will adhere to the probabilistic approach explained above for the FBM, and so we will deal with the  $\delta$ s as defined in (10) and the probabilities of (11).

Besides the three general modifications 1, 2, and 3 introduced with respect to FBMs, in order to reinforce the appearance of sudden accelerations, which constitute the genuine phenomenology of the complex aftershocks sequences, we will add two more rules for running our model.

When a breaking is going to occur in a context such that all the elements have  $\sigma < 1$ , we say that this is a normal event, the  $\delta$  is calculated using (10) and the broken element is pointed out by using (11). On the contrary, if a breaking is going to occur with one or several elements with  $\sigma \geq 1$ , we call it an avalanche step.

4. For each avalanche step, the  $\delta$  is calculated using, as usual, (10) but the element that breaks is that one whose  $\sigma_j$  surpasses 1. If there are several elements with  $\sigma > 1$ , the element that fails is that with the maximum value of  $\sigma_j$ .

5. The avalanche ends when all the  $\sigma_j$  of the set become lower than 1. During an avalanche, which in general involves several  $\delta$ , all the elements that have surpassed at any step of the avalanche the condition  $\sigma > 1$ , remain inactive with  $\sigma = 0$  until the end of the avalanche.

These two additional rules 4 and 5 are introduced in order to increase the local stress accumulations. The high stress concentrations occurring in avalanche events lead to very short  $\delta$  and in very short  $\delta$  it is reasonable to assume that there is not enough time for the healing process.

As a résumé of the above paragraphs, we will recall that in the process of evolution of the system there are normal events and avalanche events. The former (normal) refers to the failure of one element when no element in the system has  $\sigma > 1$ . The latter (avalanche

steps) corresponds to the failure of one element with  $\sigma > 1$ . Equation (10) is always used for the calculation of the time intervals. The  $\delta$  of the avalanche steps are much shorter because of the large stress concentrations induced by rules 4 and 5 and the magnitude of the exponent  $\rho$ . With these rules it is obvious that the avalanches become extinct with time because as the total stress in the system declines, it is more difficult to locally accumulate load to surpass unity. The model of Lee [1999] and Lee and Sornette [2000] cannot describe complex aftershock sequences because in their model the avalanches are instantaneous in time, so that the decay rate would have singularities at the time of an avalanche. On the contrary, our avalanches are not instantaneous since they are formed by several steps with their corresponding  $\delta$ s, that is, they occur in a finite time interval.

We have performed our simulations in a two-dimensional square lattice with 50x50 sites with  $\rho = 30$  and  $\pi = 0.7$ . Each site represents the emplacement of one element or asperity. The load transfer rule assumed is a local load-sharing (LLS) rule: a failing element trans-

fers its load to its nearest four neighbors located in the north, south, east, and west. If the element is located at the borders of the square lattice, this isotropic transfer provokes the corresponding stress leakage.

In FBMs, in which broken elements remain inactive, an LLS rule can lead to an uncertain situation when a failing element lacks active neighbors able to receive the stress transfer. In this model, though, this does not occur because any element, at any time, is active to receive stress. The only possible exceptional situation could come from the application of rule 5 in avalanches. Then the load of the failing element is transferred only to the existing active nearest neighbors. In this extremely rare case (we have not met such a situation in our simulations) of having the four nearest neighbors already broken, the load is removed from the lattice. This is just one possibility among various choices. Lomnitz-Adler *et al.* [1992] explored in detail three of these possibilities for a cellular automaton with rules similar to those of the LLS static fiber bundle model, and the reader is referred to their paper for details. In our model, deciding among one of the three alternative

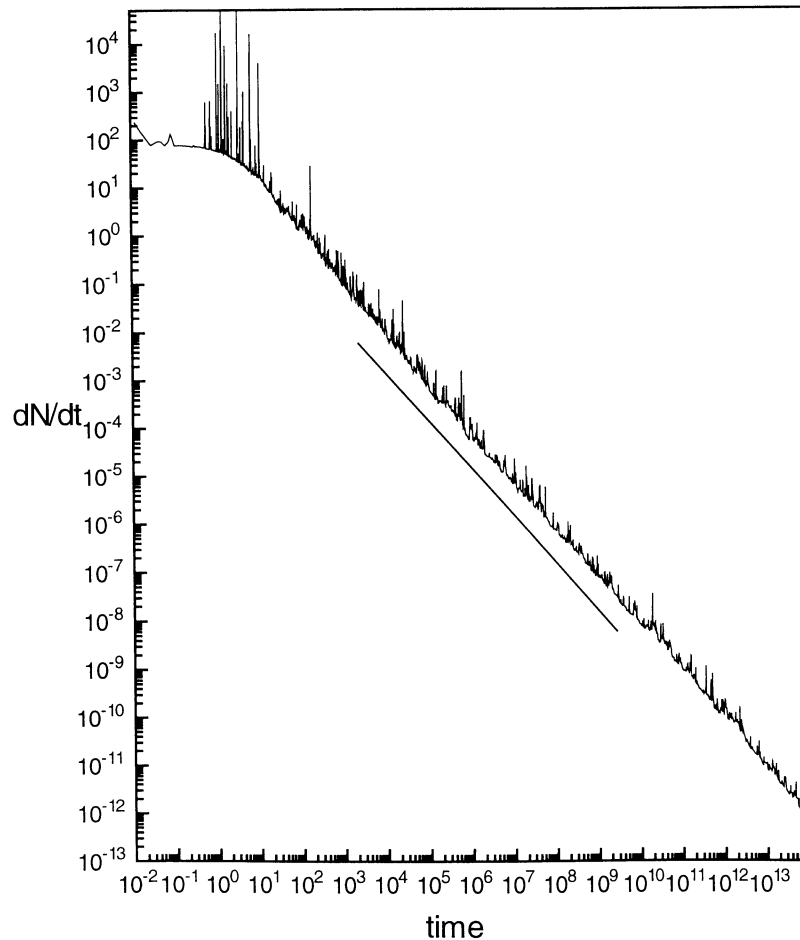


**Figure 4.** Rate of aftershocks  $dN/dt$  as a function of dimensionless time for a dissipation of  $\pi = 0.7$  and a Weibull index of  $\rho = 30$ . The spikes that decorate the general  $t^{-1}$  trend correspond to sudden accelerations in event rate (avalanches). The diagonal straight line has a slope of  $-1$ . This curve was obtained by numerically differentiating the curve in Figure 5

scenarios is not important due to the extreme rarity of such events.

The running of the program proceeds as follows. At  $t = 0$  all the elements on the lattice are initialized by loading them with a random initial stress  $\sigma_j$  taken from a uniform probability distribution  $0 \leq \sigma_j \leq 1$ . Then we calculate the  $\delta$  corresponding to the first failure by using (10). The choice of the element that actually breaks is done by using (11), and a random number between 0 and 1 to materialize the choice. The chosen element fails and  $\pi$  times its stress is transferred to its nearest neighbors and the  $(1 - \pi)$  fraction disappears. Now we analyze the distribution of stress in the board; if all the  $\sigma_i$  are lower than one, the process of calculating the next failure is identical to the first. If, on the contrary, one (or several)  $\sigma_j > 1$ , then we calculate the corresponding value of  $\delta$  from (10) and the failure is assigned to the element with the biggest  $\sigma_j > 1$ . During the period of an avalanche, rule 5 is applied to favor the stress concentration. Thus the series of breakings and transfers, involving normal events or avalanches, proceeds until a prescribed minimum value for the total stress on the system is reached, otherwise, there will be an infinite number of aftershocks.

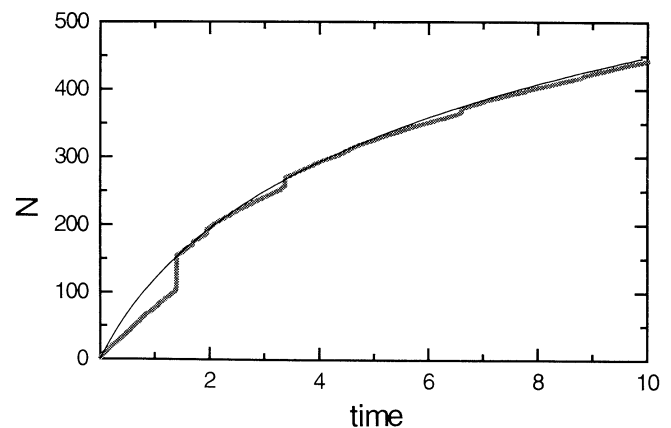
In our model, owing to the dissipation, the total stress in the system,  $S = \sum_j \sigma_j$ , systematically decreases. If the value  $\rho = 1$  were considered, then from (10) the successive  $\delta$ s would necessarily be longer and longer. However,  $\rho$  is bigger than one, and this is the reason why one can have a step down in  $S$  and find a shorter value of  $\delta$ . This is the key point to understand our model and other models based on subcritical crack growth. In the general trend of  $S$  reduction and hence temporal deceleration, the stress transfers in the system provoke local inhomogeneities in  $\sigma$ , and due to the high values of  $\rho$ , this leads to temporal accelerations. These accelerations are embedded in the general trend of dynamical relaxation.

## 5. Results and Conclusions

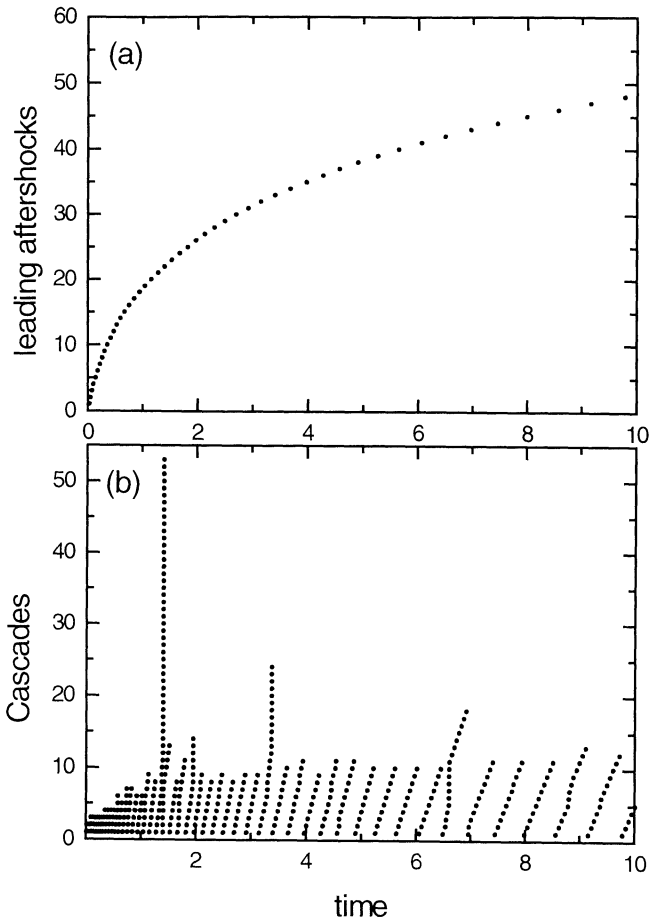
We have carried out numerical simulations which show the fulfillment of Omori's law and reproduce the features already commented on, that is, a cumulative plot with sudden variations in the number of events (accelerations). We show here the results for a two-dimensional system of  $50 \times 50$  elements located on a square lattice, with  $\rho$  equal to 30 and a conservation level of  $\pi = 0.7$ . Other simulations have also been performed varying the size of the system, the value of  $\rho$ , and the conservation level  $\pi$ . We have also explored a variant of rule 5 in which, in avalanches, all the elements with  $\sigma \geq 1$  break simultaneously in the same  $\delta$ . We have found that the results are indeed very close to those exposed here with equal qualitative behavior. Nevertheless, it should be noted that although the results are robust over a large range of parameters, different characteristics arise for extreme values of  $\rho$  and  $\pi$ .

Figure 4 shows the rate of aftershocks  $dN/dt$  as a function of time. Time is represented in dimensionless units, and it is the sum of the successive  $\delta$ s. The straight line has a slope of  $-1$  for comparison. Thus the  $1/t$  decay is confirmed and is in full agreement with Omori's law for real aftershock sequences. The depicted power law is very robust over a wide range of the parameters that characterize the model. The most critical parameter is the conservation level because for values of  $\pi$  close to unity the system does not dissipate enough to avoid its complete failure. Besides, for large dissipation  $\pi \ll 1$  the power law extends only to a few decades, and the number of decades decreases as  $\pi$  decreases. Anyhow, in all cases the exponent of the power law decay is very close to unity. The major vertical spikes of Figure 4 correspond to avalanche-type events that disappear with time. The smaller fluctuations for large times reflect the intrinsic probabilistic nature of the model and are not related at all to the appearance of avalanches. This is clearly seen in Figure 5, where we have plotted the cumulative number of aftershocks versus time instead of the differential plot of Figure 4. As can be observed in Figure 5, sudden accelerations appear in the first stages of rupture. This behavior closely resembles that previously reported in section 2 for the eastern Pyrenees aftershock sequence (see Figure 1). The Omori's law maximum likelihood fit to the model results is also included in Figure 5. The estimated parameter values are  $p = 1.01 \pm 0.06$ ,  $K = 210 \pm 29$ , and  $c = 1.3 \pm 0.2$ .

In our model the changes in aftershock rate are related to the readjustments of local stresses when events take place. With time, local concentrations of stress appear in the system, and there is a high probability of finding a region in which the load supported by the elements is close to the threshold value  $\sigma = 1$ . That is, there is a large heterogeneous stress state in which one failure will trigger an avalanche. During the evo-



**Figure 5.** Accumulated number of aftershocks  $N$  as a function of dimensionless time for a dissipation of  $\pi = 0.7$  and a Weibull index of  $\rho = 30$ . Note the sudden increases in event rate (step-like jumps) superimposed to the general Omori law trend. The continuous line is a maximum likelihood fit to the 2-10 range, and the corresponding  $p$  value is  $p = 1.01 \pm 0.06$ .



**Figure 6.** (a) Leading aftershock sequence for a simulation with  $\pi = 0.7$  and  $\rho = 30$ . (b) Model cascades. The first event in each cascade is a leading aftershock. Note that the cascades can be also approximated by straight lines, as was the case with the cascades in the actual aftershock sequence Figure 2.

lution of the avalanche the local accumulation of load increases. This fact, together with the high value of  $\rho$ , provokes the  $\delta$  corresponding to these steps of rupture to be considerably reduced. As a result, we observe the step-like change in the cumulative number of events (contrast Figure 5 with Figure 6). For large times the avalanches eventually disappear since in a nonconservative model the total load in the system systematically decreases and hence it would be unlikely to accumulate stress in local regions as to surpass the value  $\sigma = 1$ .

Of interest is the further investigation of the acceleration events in order to get an additional insight about the observed aftershock sequences. One simple way to do that was explained in section 2. It consists of decomposing the original series of aftershocks in leading events and cascades depending on whether a relaxation law is accomplished or not. We have followed the same procedure with the synthetic data. The series of cascades obtained in such a way is shown in Figure 6. Figure 6a shows the series after removing all the cascades, i.e., leaving only leading aftershocks, and in Figure 6b we plot the cascades, in which the first event of

each cascade is a leading aftershock. The decomposition obtained from the model is indeed indistinguishable from that corresponding to the real series of events (Figure 2). Two characteristics of the series of cascades are again relevant: one, the elapsed time between successive leading events is larger than the preceding one in complete agreement with the supposition of a relaxation process, and second, the series of cascades can be well approximated by almost straight segments whose slopes decrease as time passes. This later characteristic could be used to quantify the observed jumps in the cumulative plot of aftershocks and to explain why they are present mainly in the first stages of rupture. The larger jumps are related to the occurrence of avalanches, which are caused by local accumulations of stress; so it is expected that when avalanches damp out due to

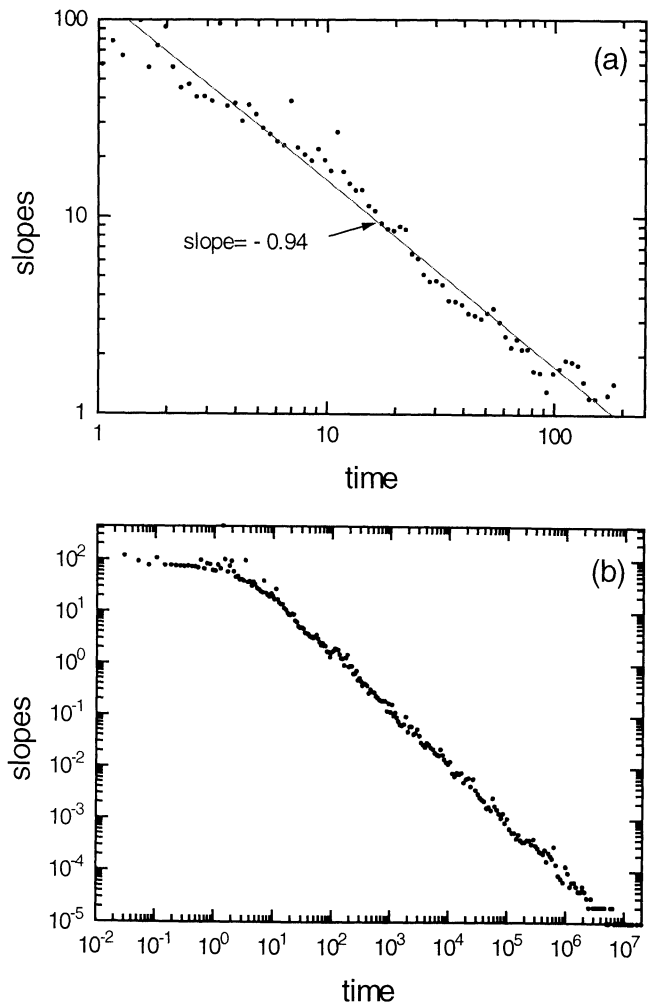


**Figure 7.** (a) Slopes of the model cascades versus dimensionless time of the leading event that initiates each cascade on log-log scale. Only the first part of the model cascades is shown in this plot to facilitate comparison with Figure 3. The local power law exponent in this part is  $\nu = 0.94$ . (b) Log-log representation of the slopes versus time for the long-time tail of the simulation. As for the eastern Pyrenees series of aftershocks the slopes fit very well a power law, in this case with an exponent of  $\sim 1.08$ .

dissipation, changes in the rate of occurrence are more spaced in time and cascades consist of fewer events. Of course, there will be fluctuations about the power law trend even in the case where avalanches have deceased. Thus we expect slope values gradually closer to zero as time tends to infinity. This is clearly appreciated in Figure 7, where we have represented in a log-log plot the slopes of the cascades versus the occurrence time of the leading event that initiate each cascade. Figure 7a shows only the first part of the time sequence to facilitate comparison with Figure 3. As for the observed series of aftershocks, the slopes fit a power law with an exponent of about  $\nu = 0.94$  for the first part of the time series and  $\nu = 1.08$  for the long-tail end Figure 7b. Actually, the long-tail exponent  $\nu$  ranges between 1.00 and 1.08 depending on the conservation level  $\pi$  and the value of  $\rho$ . This appears to be a smooth dependence. Thus the qualitative behavior is again captured. The discrepancy between the slopes ( $\nu = 0.7$  for the Pyrenees sequence) is not surprising due to the simplicity of the model as compared with the inherent complexity of the real phenomenon we want to simulate. The reason for this particular behavior, that is, why the slopes follow a power law and no other law is unclear to us up to now.

Future efforts will be devoted to the understanding of other dynamical characteristics of the model and their fine dependence on  $\rho$  and  $\pi$  by studying another complex series of aftershocks. We also plan to perform a detailed analysis of the spatial structure of the sequence of events coming from our model.

**Acknowledgments.** YM thanks the AECI for financial support. JBG thanks A.C. Cebrian for comments on maximum likelihood fitting of aftershock data. This work was supported in part by the Spanish DGICYT (Project PB98-1594).

## References

- Atkinson, B.K., Subcritical crack growth in geological materials, *J. Geophys. Res.*, *89*, 4077-4114, 1984.
- Atkinson, B.K., and P.G. Meredith, The theory of subcritical crack growth with application to minerals and rocks, In *Fracture Mechanics of Rocks*, edited by B.K. Atkinson, pp. 111-166, Academic, San Diego, Calif., 1987.
- Barnet R.L., and R. Kerrich, Stress corrosion cracking of biotite and feldspar, *Nature*, *283*, 185-187, 1980.
- Benioff, H., Earthquakes and rock creep, *Bull. Seismol. Soc. Am.*, *41*, 31-62, 1951.
- Bonn, D., H. Kellay, M. Prochnow, K. Ben-Djemaa, and J. Meunier, Delayed fracture of an inhomogeneous soft solid, *Science*, *280*, 265-267, 1998.
- Charles, R.J., Static fatigue of glass, *J. Appl. Phys.* *29*, 1549-1560, 1958.
- Coleman, B.D., Time dependence of mechanical breakdown in bundles of fibers, *J. Appl. Phys.*, *28*, 1058, 1957.
- Conchard, A., and R. Madariaga, Complexity of seismicity due to highly rate-dependent friction, *J. Geophys. Res.*, *101*, 25,321-25,336, 1996.
- Correig, A.M., M. Urquizú, J. Vila, and S. Manrubia, Aftershock series of event February 18, 1996: An interpretation in terms of self-organized criticality, *J. Geophys. Res.*, *102*, 27,407-27,420, 1997.
- Daniels, H.E., The statistical theory of the strength of bundles of threads *Proc. R. Soc. London, Ser. A*, *183*, 404, 1945.
- Das, S., and C.H. Scholz, Theory of time-dependent rupture in the Earth, *J. Geophys. Res.*, *86*, 6039-6051, 1981.
- Garcimartín, A., A. Guarino, L. Bellon, and S. Ciliberto, Statistical properties of fracture precursors, *Phys. Rev. Lett.*, *79*, 3202-3205, 1997.
- Gibowicz, S.J., An anatomy of a seismic sequence in a deep gold mine, *Pure Appl. Geophys.*, *150*, 393-414, 1997.
- Gómez, J.B., Y. Moreno, and A.F. Pacheco, Probabilistic approach to time-dependent load-transfer models of fracture, *Phys. Rev. E*, *58*, 1528-32, 1998.
- Gross, S. J., and C. Kisslinger, Tests of models of aftershock decay rate, *Bull. Seismol. Soc. Am.*, *84*, 1571- 1579, 1994.
- Hirata, T., Omori's power law aftershock sequences of microfracturing in rock fracture experiments, *J. Geophys. Res.*, *92*, 6215-21, 1987.
- Jacobs, D.S., and I.W. Chen, Mechanical and environmental factors in the cyclic and static fatigue of silicon-nitride, *J. Am. Ceram. Soc.*, *77*, 1153-1161, 1994.
- Kostrov, B.V., L.V. Nikitin, and L.M. Flitman, The mechanics of brittle fracture, *Mech. Solids*, *3*, 105-117, 1969.
- Lee, M.W., Unstable fault interactions and earthquake self-organization, Ph.D. thesis, Univ. of Calif., Los Angeles, 1999.
- Lee, M.W., and D. Sornette, Novel mechanism for discrete scale invariance in sandpile models, *Eur. Phys. J. B*, *15*, 193-197, 2000.
- Lockner, D., The role of acoustic emission in the study of rock, *Int. J. Rock Mech. Min. Sci. Geomech. Abstr.*, *30*, 883-899, 1993.
- Lockner, D., and J.D. Byerlee, Acoustic emission and creep in rocks at high confining pressures and differential stress, *Bull. Seismol. Soc. Am.*, *67*, 247-258, 1977.
- Lomnitz-Adler, J., L. Knopoff, L. and G. Martínez-Mekler, Avalanches and epidemic models of fracturing in earthquakes, *Phys. Rev. A*, *45*, 2211-2221, 1992.
- Marcellini, A., Arrhenius behavior of aftershock sequences, *J. Geophys. Res.*, *100*, 6463-6468, 1995.
- Marcellini, A., Physical model of aftershock temporal behavior, *Tectonophysics*, *277*, 137-146, 1997.
- Newman, W.I., D.L. Turcotte, and A.M. Gabrielov, Log-periodic behavior of a hierarchical failure model with applications to precursory seismic activation, *Phys. Rev. E*, *52*, 4827-35, 1995.
- Ogata, Y., Statistical models for earthquake occurrence and residual analysis for point processes, *J. Am. Stat. Assoc.*, *83*, 9-27, 1988.
- Omori, F., On after-shocks of earthquakes, *J. Coll. Sci. Imp. Univ. Tokyo*, *7*, 111-200, 1894.
- Pauchard, L., and J. Meunier, Instantaneous and time-lag breaking of a two-dimensional solid rod under a bending stress, *Phys. Rev. Lett.*, *70*, 23, 3565-68, 1993.
- Pauchet, H.A., A. Rigo, L. Rivera, and A. Sourian, A detailed analysis of the February 1996 aftershock sequence in the eastern Pyrenees, France, *Geophys. J. Int.*, *137*, 107-127, 1999.
- Phoenix, S.L., Stochastic strength and fatigue in fiber bundles, *Int. J. Fract.*, *14*, 327-344, 1977.
- Phoenix, S.L., and L. Tierney, A statistical model for the time dependent failure of unidirectional composite materials under local elastic load-sharing among fibers, *Eng. Fract. Mech.*, *18*, 193-215, 1983.
- Rigo, A., C. Olivera, A. Sourian, S. Figueras, H. Paucher, A. Grésillaud, and M. Nicolas, The February 1996 earth-

- quake sequence in the eastern Pyrenees: First results, *J. Seismol.*, *1*, 3-14, 1997.
- Sammonds, P.R., P.G. Meredith, and I.G. Main, Role of pore fluids in the generation of seismic precursors to shear fracture, *Nature*, *359*, 228-230, 1992.
- Schleinkofer, U., H.G. Sockel, K. Gorting, and W. Heinrich, Fatigue of hard metals and cermets, *Mater. Sci. Eng. A*, *209*, 313-317, 1996.
- Scholz, C.H., The frequency-magnitude relation of microfracturing in rock and its relation to earthquakes, *Bull. Seismol. Soc. Am.*, *58*, 399-415, 1968a.
- Scholz, C.H., Microfractures, aftershocks, and seismicity, *Bull. Seismol. Soc. Am.*, *58*, 1117- 30, 1968b.
- Talebi, S. (Ed.), Seismicity associated with mines, reservoirs and fluid injections, *Pure Appl. Geophys.*, *150*, 379-720, 1997.
- Utsu, T., A statistical study on the occurrence of aftershocks, *Geophys. Mag.*, *30*, 521-605, 1961.
- Utsu, T., Y. Ogata, and S Matsu'ura, The centenary of the Omori formula for a decay law of aftershock activity, *J. Phys. Earth*, *43*, 1-33, 1995.
- Vazquez-Prada, M., J.B. Gómez, Y. Moreno, and A.F. Pacheco, Time to failure of hierarchical load-transfer models of fracture, *Phys. Rev. E*, *60*, 2581-2594, 1999.
- Wennerberg, L., and R.V. Sharp, Bulk-friction of afterslip and the modified Omori law, *Tectonophysics*, *277*, 109-136, 1997.
- Wiederhorn, S.M., Influence of water vapor on crack propagation in soda-lime glass, *J. Am. Ceram. Soc.*, *50*, 407-418, 1967.
- Yamashita, T., and L. Knopoff, Model of aftershock occurrence, *Geophys. J. R. Astron. Soc.*, *91*, 13-26, 1987.
- Zhurkov, S.N., Kinetic concept of the strength of solids, *Int. J. Fract. Mech.*, *1*, 311-323, 1965.
- 
- A. Correig, Departament d'Astronomia i Meteorologia, Universitat de Barcelona, Barcelona, Spain. (e-mail: anton@am.ub.es)
- J. B. Gómez, Departamento de Ciencias de la Tierra, Universidad de Zaragoza, 50009 Zaragoza, Spain.(e-mail: jgomez@posta.unizar.es)
- Y. Moreno, The Abdus Salam International Centre for Theoretical Physics, Condensed Matter Group, Trieste, Italy. (e-mail: yamir@ictp.trieste.it)
- A. F. Pacheco, Departamento de Física Teórica, Universidad de Zaragoza, 50009 Zaragoza, Spain. (e-mail: amalio@posta.unizar.es)

(Received May 1, 2000; revised October 22, 2000; accepted October 30, 2000.)